Desalination and Water Treatment
www.deswater.com
doi: 10.5004/dwt.2023.29211

283 (2023) 237–246
January

Removal of methylene blue from aqueous solution using common bean vine and cowpea vine biomass

Guotong Qin[a], Conghui Wang[b], Qiongjie Yang[b], Wei Wei[b,*]

[a]*School of Space and Environment, Beihang University, Shahe Campus, Beijing 102206, China, Tel./Fax.: 86 10 52072157; emails: wlweiwei@buu.edu.cn (W. Wei), qingt@buaa.edu.cn (G. Qin)*
[b]*College of Biochemical Engineering, Beijing Union University, No. 18 Sanqu, Fatouxili, Chaoyang District, Beijing 100023, China, email: 181083210407@buu.edu.cn (C. Wang), 191083210415@buu.edu.cn (Q. Yang)*

Received 4 July 2022; Accepted 12 December 2022

ABSTRACT

Agricultural waste materials from common bean (*Phaseolus vulgaris* L.) and cowpea (*Vigna unguiculata* subsp. *unguiculata*) vines were investigated as adsorbents to remove methylene blue (MB) from aqueous solution. Both vines exhibited efficient adsorption of MB. Characterization of the adsorbents was performed by infrared spectroscopy, scanning electron microscopy and N_2 adsorption at 77 K. Composition was determined by the van Soest method. The adsorption isotherms of the vine adsorbents for MB fitted a Langmuir model well and the kinetics followed a pseudo-second-order model. The adsorption capacities of common bean and cowpea vines for MB were 181.82 and 144.93 mg/g, respectively, and the adsorption was a spontaneous and exothermic process. The high adsorption performance was mainly due to the hierarchical pore structure and abundant surface functional groups of the vine materials. The adsorption mechanism involved pore filling, electrostatic attraction, hydrogen bonding, π–π interactions, ion-exchange and *n*–π interactions. The results revealed that common bean and cowpea vines can be used as effective low-cost adsorbents in the treatment of contaminated wastewater.

Keywords: Biosorption; Vine biomass; Methylene blue; Exothermic; Pseudo-second-order; Langmuir model

1. Introduction

In the process of industrial treatment, about 20% of dyes are discharged into wastewater. Dye wastewater often contains dye concentrations of 10–200 mg/L [1]. Methylene blue (MB) is a cationic dye that is widely used in colorants and medicine. The dye has high chroma and is poorly biodegradable. Discharge of wastewater containing dye without treatment into bodies of water will cause serious ecological problems. There is therefore an urgent need to remove residual organic dyes from wastewater. Adsorption is an effective method to remove dyes. The capacity and cost of the adsorbent are the most important factors to determine the feasibility of an adsorption process. Activated carbon is one of the most important adsorbents in wastewater treatment, but high cost limits its application on an industrial scale. Identification of cheap, abundant, renewable adsorbents is therefore highly desirable. Recently, various agricultural solid wastes [2,3], including peel [4–8], shell [9–11], seed [12–14], husk [15–18], leaves [19–28], corn stalk [29], straw [30,31], bagasse [32] and bloom [33] have been used to remove dyes from water. Biomass adsorbent effectively reduces the cost of the adsorption process.

However, the common problem is that the adsorption capacity is still too low to scale up. Therefore, in order to increase the adsorption capacity, the biomass needs to be treated with acid or alkali.

* Corresponding author.

In China, large numbers of beans are planted, including common bean and cowpea. Because beans are grown for fruit, the vine part is usually unwanted and considered as waste. Traditionally, the vines have been discarded or burned, except for a small amount used as animal feed. However, burning of vines causes environmental pollution and has now been forbidden. Consequently, management of vine waste has become an urgent problem. Bean vines are rich in lignocelluloses that are chemically stable and suitable for use as adsorbents. However, there have been few studies on the application of bean vines as adsorbents. Only common bean waste has been used as an adsorbent to remove lead(II) ions [34,35]. Bean vines have low commercial value, so finding an industrial use for them would improve the value chain of bean production.

Herein, bean (common bean and cowpea) vines were investigated for removal of MB from water. The key process parameters affecting adsorption were studied, including MB concentration, temperature, hydraulic retention time and the solution pH. To understand the kinetics and thermodynamics of the adsorption, isotherms, kinetic models and the removal thermodynamics were elucidated.

2. Materials and methods

2.1. Chemicals and reagents

MB was obtained from Shanghai Chemical Reagent Factory (Shanghai, China). All other reagents were of analytical grade and purchased from Lanyi Chemical Reagent Company (Beijing, China).

2.2. Preparation of adsorbents

Common bean and cowpea vines were collected after harvest from a local farm (Beijing, China). The vines were washed and dried in an oven at 70°C to constant weight. The dried vines were ground and denoted as common bean vine (CBV) and cowpea vine (CV).

2.3. Characterization

The morphology and structure of the vines were analyzed by scanning electron microscopy (SEM, Sigma 300, Zeiss, Germany) and N_2 adsorption (Micromeritics ASAP 2020, USA) at 77 K. Fourier-transform infrared (FT-IR) spectroscopy (PerkinElmer, USA) was used to characterize functional groups on the vine materials. The chemical composition (cellulose, hemicellulose and lignin) of the vines was determined using the van Soest method according to the literature [36]. The pH of zero point charge (pH_{zpc}) values of the vines were determined using the method described in the literature [37].

2.4. Adsorption experiments

The vine powders (50 mg) and MB solutions (100 mL) at different concentrations were placed in 250 mL glass flasks. The flasks were shaken in a thermostatic water bath until equilibrium. The concentration of MB was determined by UV-Vis spectrophotometry (Shimadzu UV-3100, Japan) at a wavelength of 640 nm, with reference to a calibration curve. The adsorbed amount at time t, q_t (mg/g), and at equilibrium, q_e (mg/g), were calculated according to:

$$q_t = \frac{\left(C_o - C_t\right)\cdot V}{m} \tag{1}$$

$$q_e = \frac{\left(C_o - C_e\right)\cdot V}{m} \tag{2}$$

where C_o, C_t and C_e are the MB concentrations (mg/L) at start, time t and equilibrium, respectively; m (g) and V (L) represent the vine mass and MB solution volume.

2.4.1. Adsorption isotherms

The relationship between C_e and q_e was fitted using Langmuir, Freundlich and Temkin adsorption models.

The Langmuir isotherm model can be represented by the following formula [38]:

$$\frac{C_e}{q_e} = \frac{1}{q_{\max} K_L} + \frac{C_e}{q_{\max}} \tag{3}$$

where $q_{\max}$ (mg/g) is the maximum adsorption and K_L is the affinity constant, which can be obtained from the linear relationship between C_e/q_e and C_e.

The Freundlich isotherm can be written as [38]:

$$\ln q_e = \ln K_F + \frac{1}{n}\ln C_e \tag{4}$$

where the constant K_F and exponent $1/n$ can be obtained from the plot of $\ln q_e$ vs. $\ln C_e$.

The Temkin isotherm can be expressed as [38]:

$$q_e = B\ln K_T + B\ln C_e \tag{5}$$

where the constant K_T and exponent B can be calculated by plotting q_e vs. C_e.

2.4.2. Adsorption kinetics

The relationship between adsorption amount and contact time was fitted using pseudo-first-order, pseudo-second-order and intraparticle diffusion models to predict the adsorption kinetics.

The pseudo-first-order equation is expressed as follows [38]:

$$\ln\left(q_e - q_t\right) = \ln q_e - k_1 t \tag{6}$$

where k_1 (h^{-1}) is the rate constant.

The pseudo-second-order equation can be expressed as [38]:

$$\frac{t}{q_t} = \frac{1}{k_2 q_e^2} + \frac{t}{q_e} \tag{7}$$

where k_2 (g/mg·h) is the rate constant.

The intraparticle diffusion model can be represented as [38]:

$$q_t = k_i t^{1/2} + C \quad (8)$$

where k_i (mg/g·h$^{-1/2}$) is the rate constant for the intraparticle diffusion model, $t^{1/2}$ is the square root of the time and C is related to the thickness of the boundary layer.

All the tests were conducted three times and reported as the mean.

3. Results and discussion

3.1. Properties of the adsorbents

Lignin, hemicellulose and cellulose have strong adsorption capacities for dyes. Lignin has polar functional groups that can interact with cationic species, while cellulose and hemicellulose contain large numbers of hydroxyl groups that can interact via hydrogen bonding. The high specific areas of CBV and CV can provide many sites for dye adsorption [39,40]. The characterization data for CBV and CV are shown in Table 1. It can be seen that the lignin, cellulose and hemicellulose content of CBV and CV accounted for almost 50% by weight, suggesting that the materials are suitable adsorbents of dyes.

The pore structure of the adsorbent, which can be investigate by N_2 adsorption, is another important factor that affects adsorption capacity. As shown in Fig. 1a, the N_2 adsorption isotherms of CBV and CV were similar. When the relative pressure was less than 0.02, the adsorption curve was close to 0, indicating that there was no micropore structure. The hysteresis loop at relative pressures of 0.2–0.95 results from the presence of mesopores. The hysteresis loop tail at relative pressure greater than 0.95 suggests the presence of macropores. These results were confirmed by pore-size distributions (Fig. 1b), from which it can be seen that CBV and CV mainly contained mesopores and macropores, with few micropores. The Brunauer–Emmett–Teller (BET) surface areas of CBV and CV were 4.242 and 3.880 m^2/g, respectively (Table 1), which are larger than other biomass adsorbents even if those materials are subjected to a high temperature of 200°C [41,42]. High surface area is favorable for adsorption. The average pore sizes of CBV and CV were 6.44 and 6.64 nm, respectively. The molecular diameter of MB is less than 2 nm, so the pore sizes of CBV and CV are suitable for adsorption of the dye.

Table 1
Characterization of CBV and CV

Parameter	CBV	CV
Cellulose (wt.%)	31.2	29.3
Hemicellulose (wt.%)	10.9	11.1
Lignin (wt.%)	6.8	5.8
S_{BET} (m^2/g)	4.242	3.880
Pore size (nm)	6.44	6.64

The surface morphologies of CBV and CV under different SEM magnifications are shown in Fig. 2. The structures of the two vines were similar, presenting rough, heterogeneous surfaces with protuberances, cracks and cavities (Fig. 2a and e). Fig. 2b and f indicate uneven and porous structures with some elliptical holes in CBV and CV. There were also some smaller holes within the elliptical holes. Fig. 2c and g show that the vine materials had particulate forms with irregular shapes and heterogeneous cavities at the mesoporous scale. These results are consistent with the nitrogen adsorption data. The macropores and mesopores increase the surface area of the adsorbents, which is conducive to adsorption of dye molecules. At the same time, the large pore size enables fast diffusion of dye molecules and shortens adsorption equilibration time. After adsorption, MB molecules fill the pores and cover the surfaces of the adsorbents (Fig. 2d and h) which shows MB dye molecules are evenly distributed on the surface of CBV and CV. The same phenomenon occurs when MB is adsorbed on the surface of activated carbon [43].

The pH_{zpc} values of CBV and CV, which were 5.9 and 6.0, respectively (Fig. 3a), were determined to understand their surface charge properties.

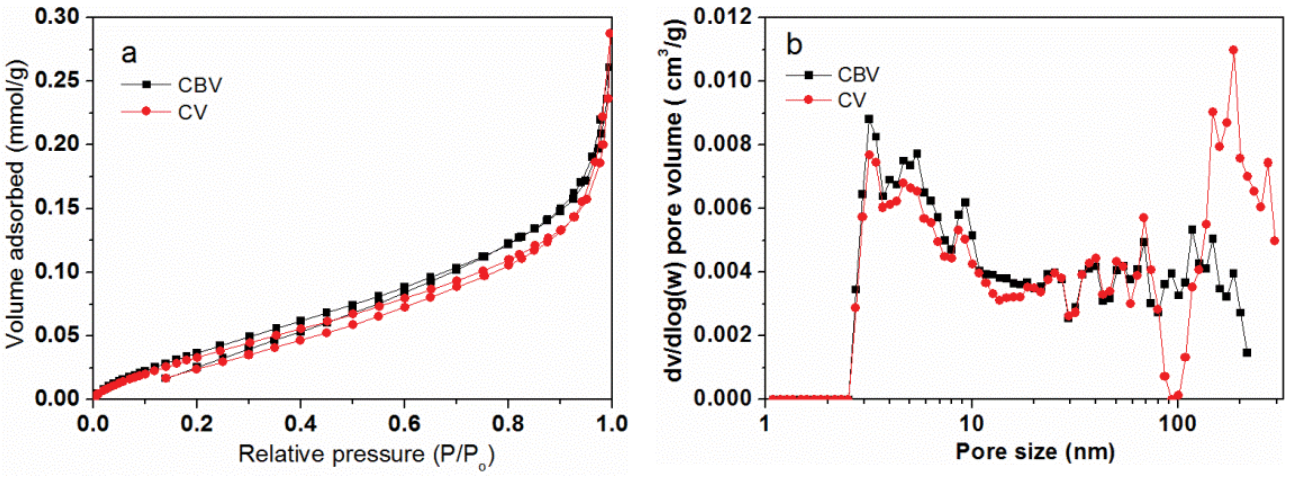

Fig. 1. The N_2 adsorption isotherm patterns (a) and pore-size distributions (b) of CBV and CV.

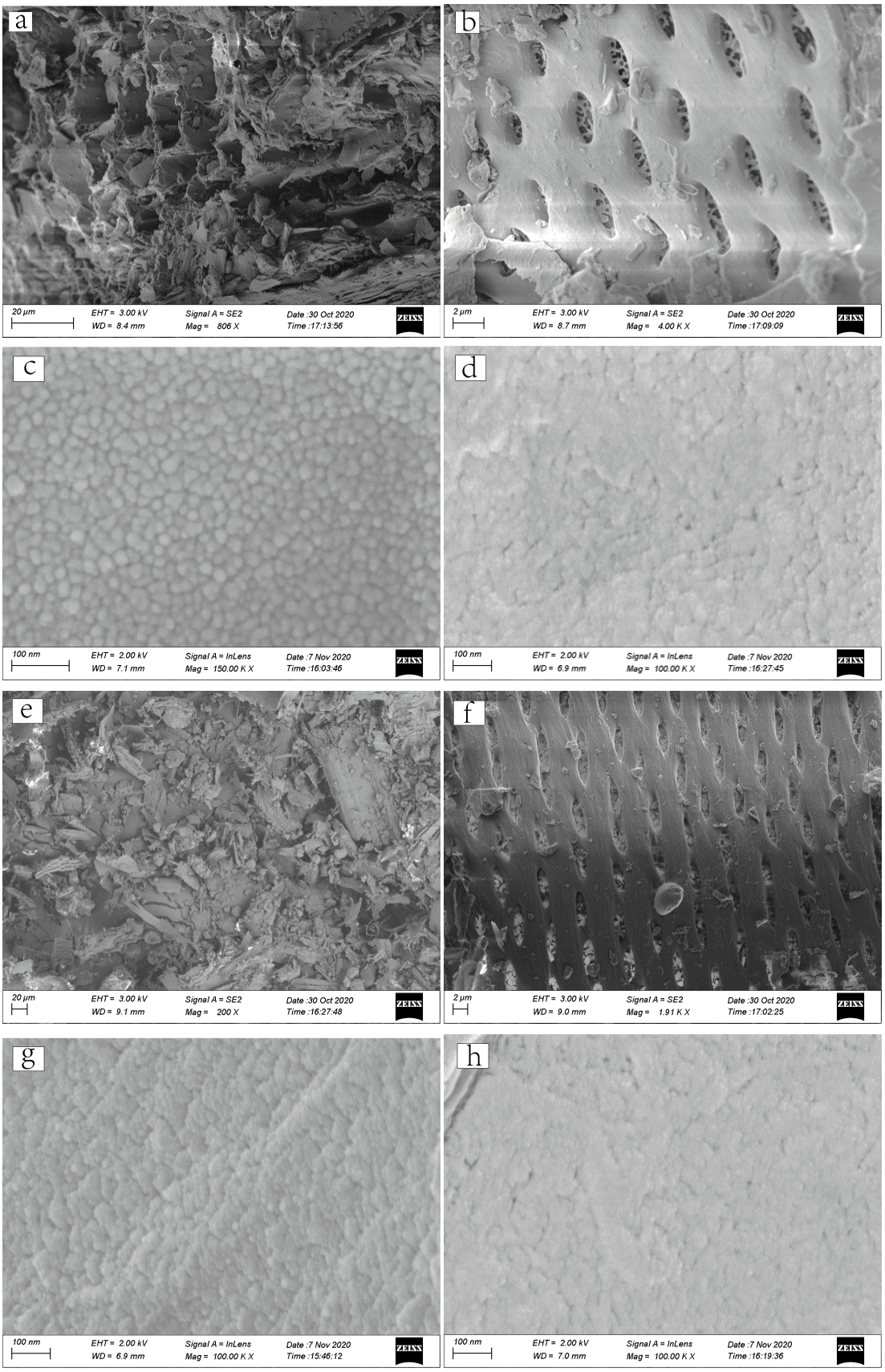

Fig. 2. SEM images of the CBV (a–d) and CV (e–h) adsorbents before (a–c, e–g) and after (d, h) adsorption.

3.2. Adsorption performance analysis

3.2.1. Adsorption kinetics

The adsorption rate is important for determining the utility of an adsorbent. Fig. 4 shows the effect of contact time on the adsorption of MB by CBV and CV at 30°C. Within 5 min, the amount adsorbed rapidly exceeded 50% of the total adsorption capacity for various initial dye concentrations. Equilibrium was reached within 120 min. The rapid adsorption of MB by CBV and CV was mainly due to the large pore size and abundant adsorption sites on the surfaces of the adsorbents. The adsorption capacities of CBV and CV decreased as the initial MB concentration was decreased. Three kinetic models, pseudo-first-order, pseudo-second-order, and intraparticle diffusion, were used to explore the underlying mechanisms of MB adsorption. It was found that MB adsorption best fitted the pseudo-second-order model and the corresponding parameters are listed in Table 2.

3.2.2. Effects of concentration and temperature

To investigate the effects of MB concentration and adsorption temperature, the adsorption capacities of both CBV and CV were studied at different temperatures and with different initial MB concentrations (Fig. 5). The results indicated slightly higher adsorption by CBV than CV, probably due its higher lignocellulose content and higher BET surface area. The adsorption capacity was enhanced at lower temperatures. Langmuir, Freundlich and Temkin models were used to explore the mechanisms of MB adsorption by CBV and CV. The Langmuir model postulates a monolayer adsorption process in which the pore can accept only one MB dye molecule. The Freundlich model assumes that the adsorption surface is non-uniform and that adsorption is a nonlinear process. Temkin considers the interaction between adsorbate and adsorbent and assumes that the adsorption free energy is the only function of surface coverage.

The Langmuir model described the results well, with $R^2 > 0.99$, and the model parameters are listed in Table 3. This result indicated that adsorption of MB dye by CBV and CV was a monolayer-molecular adsorption process. The q_{max} values for MB on CBV and BV were 181.82 and 149.25 mg/g at 30°C, respectively.

The change of Gibbs free energy, entropy ($\Delta S°$) and enthalpy ($\Delta H°$) were determined to better estimate the effect

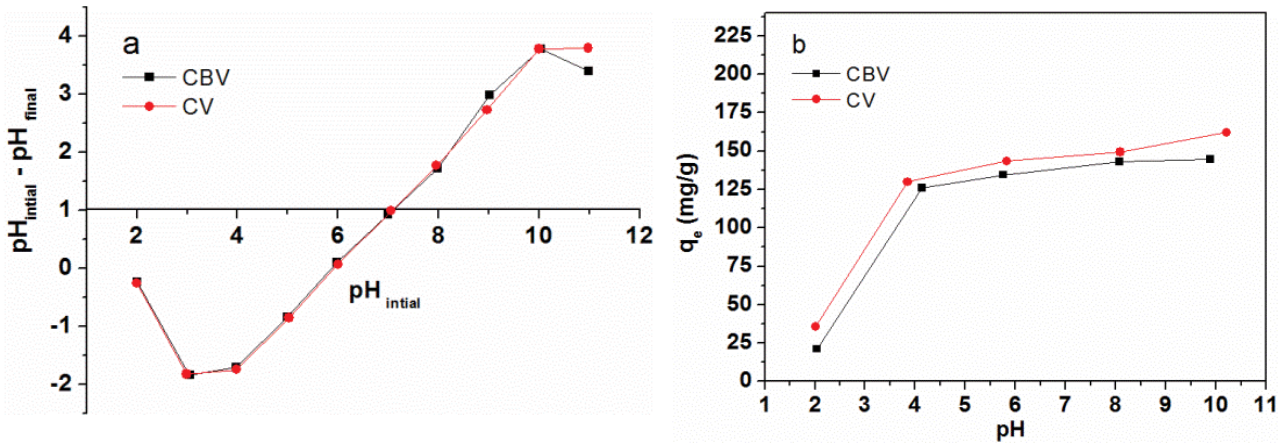

Fig. 3. Plots of pH_{zpc} of vines (a) and the effects of pH on the MB adsorption by vines (b).

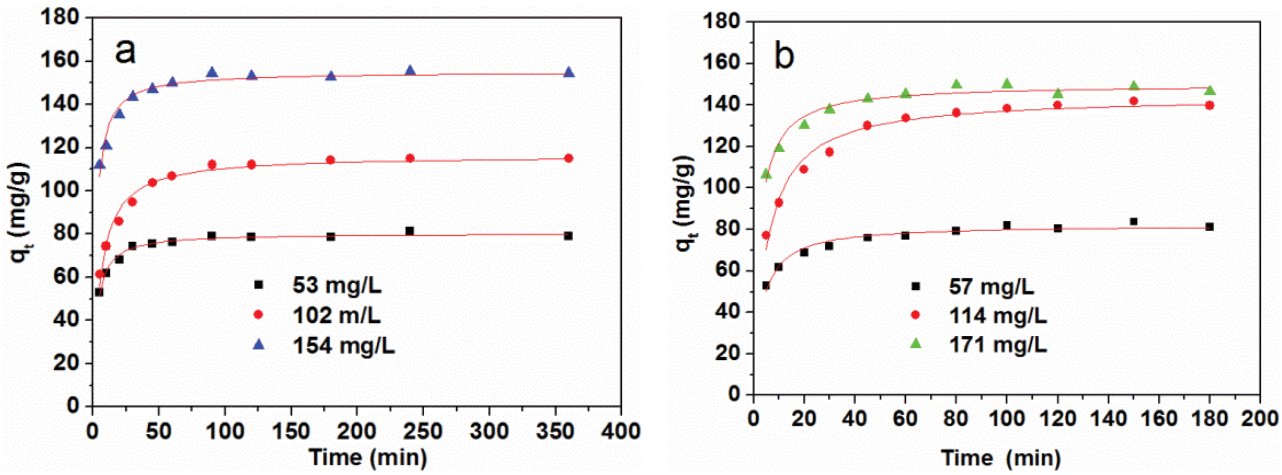

Fig. 4. Effects of the contact time on the adsorption of MB by CBV (a) and CV (b).

Table 2
Parameters from the pseudo-second-order model of MB adsorption by CBV and CV

Sample	Initial concentration (mg/L)	Parameters			
		$q_{e(exp)}$ (mg/g)	$k_2 \times 10^4$ (min)	$q_{e(cal)}$ (mg/g)	R^2
CBV	53.6	80.00	28.52	81.23	0.999
	106.4	132.56	7.71	135.32	0.999
	177.6	157.91	24.5	158.73	0.999
CV	57.9	82.22	29.99	83.75	0.999
	106.4	112.00	11.26	116.96	0.999
	172.1	134.13	9.13	139.86	0.999

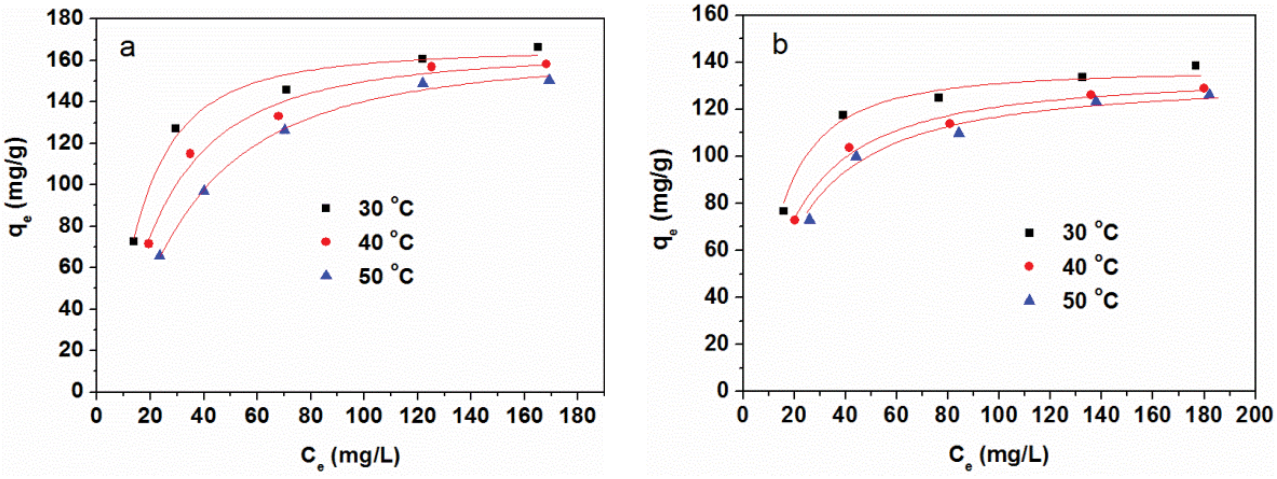

Fig. 5. Adsorption isotherms obtained for MB on CBV (a) and CV (b).

Table 3
Langmuir isotherm constants obtained for the adsorption of MB using CBV and CV

Sample	Temperature (°C)	Langmuir		
		q_{max} (mg/g)	K_L (L/mg) × 10^{-2}	R^2
CBV	30	181.82	5.95	0.995
	40	178.57	5.05	0.995
	50	175.75	3.83	0.998
CV	30	149.25	7.49	0.999
	40	142.05	5.54	0.999
	50	141.84	4.49	0.998

of temperature on adsorption of MB by the adsorbents. The equilibrium constants K_L from the Langmuir equation at 30°C, 40°C and 50°C were used to calculate these thermodynamic parameters [44]{Ahmad, 2011 #27}.

The free energy change of adsorption is given as:

$$\Delta G^\circ = \Delta H^\circ - T\Delta S^\circ \quad (9)$$

$$\Delta G^\circ = -RT \ln K_L \quad (10)$$

where T is the temperature (K), and R is the ideal gas constant (8.314 J/mol K); ΔH° and ΔS° were obtained by plotting $\ln K_L$ vs. $1/T$ [45].

The calculated entropies, free energies and enthalpies of MB adsorption are presented in Table 4. The decrease of Gibbs free energy ($\Delta G^\circ < 0$) suggests that the adsorption is spontaneous. The negative value of ΔH° indicates that uptake of MB is exothermic. This is also supported by the increase of MB adsorption capacity as the temperature was decreased [46]. The increase of entropy ($\Delta S^\circ > 0$) indicates that disorder at the liquid/solid interface is increased after adsorption.

3.2.3. Effect of pH and adsorption mechanism

Generally, adsorption involves electrostatic attraction, pore filling, ion-exchange, hydrogen-bonding, π–π interactions, and *n*–π interactions. Pore filling participates in the adsorption of MB by CBV and CV, which can be seen in Fig. 2. The pH of the MB solution affects the charge on the adsorbent surface and the aqueous chemical properties, which influence the adsorption process. The adsorption behaviors of CBV and CV were measured at pH values of 2–10 and the results are shown in Fig. 3b. The uptake of MB increased as the pH was increased. The increase was most obvious at pH 2–6. The pH_{zpc} values of CBV and CV were 5.9 and 6.1, respectively. When the pH of the solution is below pH_{zpc}, the surfaces of CBV and CV are positively charged, resulting in strong electrostatic repulsion of cationic MB and decreased dye uptake. When the pH is above pH_{zpc}, the surfaces of CBV and CV are negatively charged, resulting in strong electrostatic attraction of MB and increased dye uptake. Therefore, electrostatic attraction has a pivotal role in the adsorption of MB by CBV and CV. Since positively charged MB is still adsorbed by positively charged CBV and CV (at $pH < pH_{zpc}$), ion-exchange may also be involved in the adsorption [47].

The FT-IR spectra of CBV and CV before and after dye adsorption are presented in Fig. 6. The spectra showed a broad peak at 3,402 cm^{-1} (O–H stretching vibration in carboxylic acid groups) together with peaks at 2,922 cm^{-1} (aliphatic C–H stretching), 1,743 cm^{-1} (C=O stretch of ketones, lactones, and carboxylic anhydrides), 1,612 and 1,635 cm^{-1} (C=C olefin stretch), 1,423 cm^{-1} (O–H in-plane bending in carboxylic acid groups), 1,245 cm^{-1} (C–N stretching vibration in amines) and 1,077 cm^{-1} (C–N stretching vibration in amines) [22]. The O–H, C–N and C=O groups participate in the adsorption process, providing crucial sites for MB location [40]. In addition, previous studies have shown that such polar groups are conducive to adsorption of cationic dye by electrostatic interaction [47]. The surfaces of CBV and CV have hydroxyl groups that can form hydrogen bonds. In addition, *n*–π interactions may be formed between hydroxyl groups and the aromatic ring of MB [30]. All of these interactions increase the adsorption capacity. After adsorption, the peaks due to C=C became deeper and shifted from 1,612 and 1,635 to 1,601 cm^{-1}.This change suggests π–π interactions between benzene rings in MB molecules occur and that formation of a conjugated structure in CBV and CV is conducive to adsorption [15,48]. New peaks at 1,386 cm^{-1} (C=N stretching vibration) and 1,328 cm^{-1} (N–H stretching vibration) were formed after adsorption, which indicates that MB was adsorbed.

Table 5 compares MB removal capacities of CBV and CV with those of bioadsorbents derived from various plants published in the literature. The removal capacities of CBV and CV were higher than those of most reported bioadsorbents. Consequently, CBV and CV appear to have enormous potential as dye adsorbents.

4. Conclusions

In this study, MB was effectively removed from aqueous solution by CBV and CV. The pore structure of the vine materials and functional groups on their surfaces contribute to good adsorption. Contact temperature, time, MB concentration and solution pH affected the adsorption process. Adsorption of MB by CBV and CV followed the pseudo-second-order and Langmuir isotherm models, demonstrating that the adsorption process is a monolayer adsorption. The maximum adsorption capacity of CBV and CV reached 181.82 and 149.25 mg/g at 30°C, respectively. The decrease of Gibbs free energy and negative value of Δ*H* indicate that adsorption of MB is spontaneous and exothermic. As renewable, low-cost, waste agricultural by-products with good adsorption capacities for MB, CBV and CV are economical and practicable in the field of wastewater treatment.

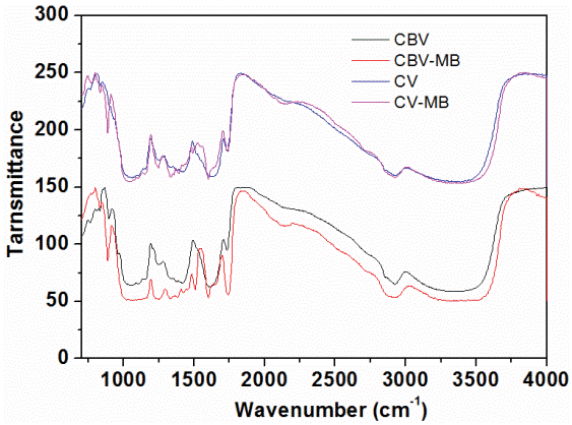

Fig. 6. FT-IR spectra obtained for CBV and CV before and after the adsorption of methylene blue from an aqueous solution.

Table 4
Thermodynamic parameters obtained for the adsorption of MB using CBV and CV

Samples	Temperature (°C)	ΔG° (kJ/mol)	Δ*S*° (J/mol·K)	Δ*H*° (kJ/mol)
CBV	30	−27.695	32.425	−17.922
	40	−28.182		
	50	−28.339		
CV	30	−28.274	24.493	−20.815
	40	−28.423		
	50	−28.767		

Table 5
Comparison of the MB removal capacity of various bioadsorbents

Bioadsorbent	MB removal capacity (mg/g)	References
Acid-washed black cumin seed material	73.529	[14]
Pine seed	110	[49]
Walnut bloom	46	[33]
Rice husk powder	50.15	[15]
Green tea waste	69.01	[27]
Syringa vulgaris leaf	188.2	[28]
De-oiled soya solid coated with silica	88.4	[47]
Organosolv lignin from rice straw	40.02	[50]
Soursop	42.1417	[2]
Walnut shell	196.078	[11]
Tobacco stem biomass	169.5	[51]
Cauliflower leaf powder	149.22	[26]
Carrot leaf powder	66.6	[52]
Carrot stem powder	55.5	[52]
Chitosan/nano-lignin from palm kernel shell	74.07	[53]
Biocomposite beads (from sodium alginate and waste after oil extraction of almond and peanut)	22.8	[54]
Ulva fasciata	244	[55]
Sargassum dentifolium	66.6	[55]
Tannins immobilized on cellulose microfibers	31.7	[56]
Sulfosalicylic acid-modified lignin	83.2	[57]
Casuarina equisetifolia pines	41.35	[58]
Chlorophyceae	94.76	[59]
Coconut leaves	112.35	[19]
Watermelon rinds	188.68	[4]
Banana peels	250	[5]
Rice straw	158	[30]
CBV	181.82	This work
CV	149.25	This work

Acknowledgments

This work was supported by the Natural Science Foundation of China (No. 51772031).

References

[1] S. Chakraborty, S. Chowdhury, P. Das Saha, Adsorption of Crystal Violet from aqueous solution onto NaOH-modified rice husk, Carbohydr. Polym., 86 (2011) 1533–1541.
[2] L. Meili, P.V.S. Lins, M.T. Costa, R.L. Almeida, A.K.S. Abud, J.I. Soletti, G.L. Dotto, E.H. Tanabe, L. Sellaoui, S.H.V. Carvalho, A. Erto, Adsorption of methylene blue on agroindustrial wastes: experimental investigation and phenomenological modelling, Prog. Biophys. Mol. Biol., 141 (2019) 60–71.
[3] H. Aghdasinia, M. Gholizadeh, S.S. Hosseini, Adsorptive removal of basic yellow 2 onto reed stem and poplar leaf: a comprehensive study, Sustainable Chem. Pharm., 24 (2021) 100546, doi: 10.1016/j.scp.2021.100546.
[4] A.H. Jawad, Y.S. Ngoh, K.A. Radzun, Utilization of watermelon (*Citrullus lanatus*) rinds as a natural low-cost biosorbent for adsorption of methylene blue: kinetic, equilibrium and thermodynamic studies, J. Taibah Univ. Sci., 12 (2018) 371–381.
[5] A.H. Jawad, R. Abd Rashid, M.A.M. Ishak, K. Ismail, Adsorptive removal of methylene blue by chemically treated cellulosic waste banana (*Musa sapientum*) peels, J. Taibah Univ. Sci., 12 (2018) 809–819.
[6] S. Rani, S. Chaudhary, Adsorption of methylene blue and crystal violet dye from waste water using *Citrus limetta* peel as an adsorbent, Mater. Today Proc., 60 (2022) 336–344.
[7] F. Abdelghaffar, Biosorption of anionic dye using nanocomposite derived from chitosan and silver nanoparticles synthesized via cellulosic banana peel bio-waste, Environ. Technol. Innovation, 24 (2021) 101852, doi: 10.1016/j.eti.2021.101852.
[8] R. Rehman, A. Jamil, F. Alakhras, Sorptive removal of diamond green dye by acid treated *Punica granatum* peels in eco-friendly way, Int. J. Phytorem., 24 (2022) 245–254.
[9] Y.I. Coskun, Investigation of adsorption performances of green walnut hulls for the removal of methylene blue, Desal. Water Treat., 247 (2022) 281–293.
[10] Y.H. Song, R. Peng, L.L. Gou, M. Ye, Removal of sunset yellow by methanol modified walnut shell, Iran. J. Chem. Chem. Eng.-Int. Engl. Ed., 40 (2021) 1095–1104.
[11] Y. Miyah, A. Lahrichi, M. Idrissi, A. Khalil, F. Zerrouq, Adsorption of methylene blue dye from aqueous solutions onto walnut shells powder: equilibrium and kinetic studies, Surf. Interfaces, 11 (2018) 74–81.
[12] A. Goyal, P. Singh, P. Chamoli, K.K. Raina, R.K. Shukla, Eco-friendly biowaste-based natural surfactant for lyotropic

assemblies and bio-adsorbent for dye removal, Inorg. Chem. Commun., 133 (2021) 108871, doi: 10.1016/j.inoche.2021.108871.
[13] Y. Akköz, R. Coşkun, A. Delibaş, Preparation and characterization of sulphonated bio-adsorbent from waste hawthorn kernel for dye (MB) removal, J. Mol. Liq., 287 (2019) 110988, doi: 10.1016/j.molliq.2019.110988.
[14] S.I. Siddiqui, G. Rathi, S.A. Chaudhry, Acid washed black cumin seed powder preparation for adsorption of methylene blue dye from aqueous solution: thermodynamic, kinetic and isotherm studies, J. Mol. Liq., 264 (2018) 275–284.
[15] X. You, R. Wang, Y. Zhu, W. Sui, D. Cheng, Comparison of adsorption properties of a cellulose-rich modified rice husk for the removal of methylene blue and aluminum(III) from their aqueous solution, Ind. Crops Prod., 170 (2021) 113687, doi: 10.1016/j.indcrop.2021.113687.
[16] V.V. Dev, B. Wilson, K.K. Nair, S. Antony, K.A. Krishnan, Response surface modeling of Orange-G adsorption onto surface tuned ragi husk, Colloid Interface Sci. Commun., 41 (2021) 100363, doi: 10.1016/j.colcom.2021.100363.
[17] A. Dar, A. Safdar, J. Anwar, Removal of anionic dye from industrial effluents with raw and chemically modified chickpea husk, J. Chem. Soc. Pak., 40 (2018) 319–326.
[18] K.K. Hummadi, S. Luo, S. He, Adsorption of methylene blue dye from the aqueous solution via bio-adsorption in the inverse fluidized-bed adsorption column using the torrefied rice husk, Chemosphere, 287 (2022) 131907, doi: 10.1016/j.chemosphere.2021.131907.
[19] A.H. Jawad, R. Abd Rashid, R.M.A. Mahmuod, M.A.M. Ishak, N.N. Kasim, K. Ismail, Adsorption of methylene blue onto coconut (*Cocos nucifera*) leaf: optimization, isotherm and kinetic studies, Desal. Water Treat., 57 (2016) 8839–8853.
[20] H.S. AL-Shehri, H.S. Alanazi, A.M. Shaykhayn, L.S. ALharbi, W.S. Alnafaei, A.Q. Alorabi, A.S. Alkorbi, F.A. Alharthi, Adsorption of methylene blue by biosorption on alkali-treated *Solanum incanum*: isotherms, equilibrium and mechanism, Sustainability, 14 (2022) 2644, doi: 10.3390/su14052644.
[21] Z. Recber, Adsorption of methylene blue onto spent alchemilla vulgaris leaves: characterization, isotherms, kinetic and thermodynamic studies, Int. J. Environ. Sci. Technol., 19 (2022) 4803–4814.
[22] R. Das, A. Mukherjee, I. Sinha, K. Roy, B.K. Dutta, Synthesis of potential bio-adsorbent from Indian Neem leaves (*Azadirachta indica*) and its optimization for malachite green dye removal from industrial wastes using response surface methodology: kinetics, isotherms and thermodynamic studies, Appl. Water Sci., 10 (2020) 117, doi: 10.1007/s13201-020-01184-5.
[23] K. Ghosh, N. Bar, A.B. Biswas, S.K. Das, Removal of methylene blue (aq) using untreated and acid-treated eucalyptus leaves and GA-ANN modelling, Can. J. Chem. Eng., 97 (2019) 2883–2898.
[24] P. Boonsong, J. Paksamut, Efficiency improvement of some agricultural residue modified materials for textile dyes absorption, IOP Conf. Ser.: Mater. Sci. Eng., 317 (2018) 012035.
[25] F. Tang, Y.Y. Li, Y.M. Zhao, Q. Zhou, Y.Z. Peng, Enhanced removal of methyl violet using NaOH-modified *C. camphora* leaves powder and its renewable adsorption, Desal. Water Treat., 98 (2017) 306–314.
[26] S.A. Ansari, F. Khan, A. Ahmad, Cauliflower leave, an agricultural waste biomass adsorbent, and its application for the removal of MB dye from aqueous solution: equilibrium, kinetics, and thermodynamic studies, Int. J. Anal. Chem., 2016 (2016) 8252354, doi: 10.1155/2016/8252354.
[27] M. El-Azazy, A.S. El-Shafie, B. Al-Shaikh Yousef, Green tea waste as an efficient adsorbent for methylene blue: structuring of a novel adsorbent using full factorial design, Molecules, 26 (2021) 6138, doi: doi: 10.3390/molecules26206138.
[28] G. Mosoarca, C. Vancea, S. Popa, M. Gheju, S. Boran, *Syringa vulgaris* leaves powder a novel low-cost adsorbent for methylene blue removal: isotherms, kinetics, thermodynamic and optimization by Taguchi method, Sci. Rep., 10 (2020) 17676, doi: 10.1038/s41598-020-74819-x.
[29] Y. Tang, Y. Zhao, T. Lin, Y. Li, R. Zhou, Y. Peng, Adsorption performance and mechanism of methylene blue by H_3PO_4-modified corn stalks, J. Environ. Chem. Eng., 7 (2019) 103398, doi: 10.1016/j.jece.2019.103398.
[30] A.H. Jawad, N. Hum, A.M. Farhan, M.S. Mastuli, Biosorption of methylene blue dye by rice (*Oryza sativa* L.) straw: adsorption and mechanism study, Desal. Water Treat., 190 (2020) 322–330.
[31] Y. Shang, J. Zhang, X. Wang, R. Zhang, W. Xiao, S. Zhang, R. Han, Use of polyethyleneimine-modified wheat straw for adsorption of Congo red from solution in batch mode, Desal. Water Treat., 57 (2016) 8872–8883.
[32] L.W. Low, T.T. Teng, N. Morad, B. Azahari, Studies on the Adsorption of Methylene Blue Dye from Aqueous Solution onto Low-Cost Tartaric Acid Treated Bagasse, 3rd Int. Conf. Environ. Sci. Dev. (ICESD), Hong Kong, Peoples R China, 2012, pp. 103–109.
[33] E.M. Khosrowshahi, N. Farhami, B. Jannat, S. Farrokhzadeh, H. Razmi, Walnut bloom powder as a waste-based sorbent for cationic dyes removal: equilibrium, kinetic, and thermodynamic studies, Can. J. Chem., 99 (2021) 956–963.
[34] A. Safa Özcan, S. Tunali, T. Akar, A. Özcan, Biosorption of lead(II) ions onto waste biomass of *Phaseolus vulgaris* L.: estimation of the equilibrium, kinetic and thermodynamic parameters, Desalination, 244 (2009) 188–198.
[35] M. Ferreira, P.S.M. Santos, M.T.M. Caldeira, A.C. Estrada, J.P.D. Costa, T.A.P. Rochasantos, A.C. Duarte, White bean (*Phaseolus vulgaris* L.) as a sorbent for the removal of zinc from rainwater, Water Res., 162 (2019) 170–179.
[36] A. Bartos, J. Anggono, Á.E. Farkas, D. Kun, F.E. Soetaredjo, J. Móczó, Antoni, H. Purwaningsih, B. Pukánszky, Alkali treatment of lignocellulosic fibers extracted from sugarcane bagasse: composition, structure, properties, Polym. Test., 88 (2020) 106549, doi: 10.1016/j.polymertesting.2020.106549.
[37] M.A. Islam, M.J. Ahmed, W.A. Khanday, M. Asif, B.H. Hameed, Mesoporous activated coconut shell-derived hydrochar prepared via hydrothermal carbonization-NaOH activation for methylene blue adsorption, J. Environ. Manage., 203 (2017) 237–244.
[38] M. Rajabi, B. Mirza, K. Mahanpoor, M. Mirjalili, F. Najafi, O. Moradi, H. Sadegh, R. Shahryari-ghoshekandi, M. Asif, I. Tyagi, S. Agarwal, V.K. Gupta, Adsorption of malachite green from aqueous solution by carboxylate group functionalized multi-walled carbon nanotubes: determination of equilibrium and kinetics parameters, J. Ind. Eng. Chem., 34 (2016) 130–138.
[39] S. Dridi-Dhaouadi, N.B. Douissa-Lazreg, M.F. M'Henni, Removal of lead and Yellow 44 acid dye in single and binary component systems by raw *Posidonia oceanica* and the cellulose extracted from the raw biomass, Environ. Technol., 32 (2011) 325–340.
[40] D. Castro, N.M. Rosas-Laverde, M.B. Aldás, C.E. Almeida-Naranjo, V.H. Guerrero, A.I. Pruna, Chemical modification of agro-industrial waste-based bioadsorbents for enhanced removal of Zn(II) ions from aqueous solutions, Materials, 14 (2021) 2134, doi: 10.3390/ma14092134.
[41] S. Liu, J. Li, S. Xu, M. Wang, Y. Zhang, X. Xue, A modified method for enhancing adsorption capability of banana pseudostem biochar towards methylene blue at low temperature, Bioresour. Technol., 282 (2019) 48–55.
[42] J. Ma, D. Huang, J. Zou, L. Li, Y. Kong, S. Komarneni, Adsorption of methylene blue and Orange II pollutants on activated carbon prepared from banana peel, J. Porous Mater., 22 (2015) 301–311.
[43] A.H. Jawad, M. Bardhan, M.A. Islam, M.A. Islam, S.S.A. Syed-Hassan, S.N. Surip, Z.A. Alothman, M.R. Khan, Insights into the modeling, characterization and adsorption performance of mesoporous activated carbon from corn cob residue *via* microwave-assisted H_3PO_4 activation, Surf. Interfaces, 21 (2020) 100688, doi: 10.1016/j.surfin.2020.100688.
[44] O.S. Bello, B.M. Lasisi, O.J. Adigun, V. Ephraim, Scavenging Rhodamine B dye using moringa oleifera seed pod, Chem. Speciation Bioavailability, 29 (2017) 120–134.

[45] S.K. Milonjic, A consideration of the correct calculation of thermodynamic parameters of adsorption, J. Serb. Chem. Soc., 72 (2007) 1363–1367.
[46] Z. Jiang, D. Hu, Molecular mechanism of anionic dyes adsorption on cationized rice husk cellulose from agricultural wastes, J. Mol. Liq., 276 (2019) 105–114.
[47] A. Batool, S. Valiyaveettil, Chemical transformation of soya waste into stable adsorbent for enhanced removal of methylene blue and neutral red from water, J. Environ. Chem. Eng., 9 (2021) 104902, doi: 10.1016/j.jece.2020.104902.
[48] R. Lin, Z. Liang, C. Yang, Z. Zhao, F. Cui, Selective adsorption of organic pigments on inorganically modified mesoporous biochar and its mechanism based on molecular structure, J. Colloid Interface Sci., 573 (2020) 21–30.
[49] A. Mohmoud, F. Kooli, Y. Liu, Waste of pine seeds as bio-removal agent for methylene blue from aqueous solution: regeneration and single-stage batch design, Desal. Water Treat., 204 (2020) 144–154.
[50] S. Zhang, Z. Wang, Y. Zhang, H. Pan, L. Tao, Adsorption of methylene blue on organosolv lignin from rice straw, Procedia Environ. Sci., 31 (2016) 3–11.
[51] D.D. Reddy, R.K. Ghosh, J.P. Bindu, M. Mahadevaswamy, T.G.K. Murthy, Removal of methylene blue from aqueous system using tobacco stems biomass: kinetics, mechanism and single-stage adsorber design, Environ. Prog. Sustainable Energy, 36 (2017) 1005–1012.
[52] A.K. Kushwaha, N. Gupta, M.C. Chattopadhyaya, Removal of cationic methylene blue and malachite green dyes from aqueous solution by waste materials of *Daucus carota*, J. Saudi Chem. Soc., 18 (2014) 200–207.
[53] S. Sohni, R. Hashim, H. Nidaullah, J. Lamaming, O. Sulaiman, Chitosan/nano-lignin based composite as a new sorbent for enhanced removal of dye pollution from aqueous solutions, Int. J. Biol. Macromol., 132 (2019) 1304–1317.
[54] M. Erfani, V. Javanbakht, Methylene blue removal from aqueous solution by a biocomposite synthesized from sodium alginate and wastes of oil extraction from almond peanut, Int. J. Biol. Macromol., 114 (2018) 244–255.
[55] R.M. Moghazy, A. Labena, S. Husien, Eco-friendly complementary biosorption process of methylene blue using micro-sized dried biosorbents of two macro-algal species (*Ulva fasciata* and *Sargassum dentifolium*): full factorial design, equilibrium, and kinetic studies, Int. J. Biol. Macromol., 134 (2019) 330–343.
[56] G. Wang, Y. Chen, G. Xu, Y. Pei, Effective removing of methylene blue from aqueous solution by tannins immobilized on cellulose microfibers, Int. J. Biol. Macromol., 129 (2019) 198–206.
[57] Y. Jin, C. Zeng, Q.-F. Lü, Y. Yu, Efficient adsorption of methylene blue and lead ions in aqueous solutions by 5-sulfosalicylic acid modified lignin, Int. J. Biol. Macromol., 123 (2019) 50–58.
[58] H. Chandarana, P. Senthil Kumar, M. Seenuvasan, M. Anil Kumar, Kinetics, equilibrium and thermodynamic investigations of methylene blue dye removal using *Casuarina equisetifolia* pines, Chemosphere, 285 (2021) 131480, doi: 10.1016/j.chemosphere.2021.131480.
[59] B.M. Seth, V. Uniyal, D. Kumar, A. Singh, Sorption of cationic and anionic dyes by dead biomass of filamentous green alga *Cladophora* sp. (*Chlorophyceae*), Int. J. Environ. Sci. Technol., 19 (2022) 12079–12090.